

CURRENT AND FUTURE ASPECTS OF CANCER DIAGNOSIS WITH POSITRON EMISSION TOMOGRAPHY

T. Matsuzawa

M. Tada, H. Fukuda, Y. Abe, T. Fujiwara, M. Itoh, J. Hatazawa, K. Kubota, K. Yamaguchi, K. Itoh, T. Satoh, Y. Sugawara, T. Ido*, R. Iwata*, K. Ishiwata*, T. Takahashi*, M. Monma*, H. Orihara**, K. Ishii**, and S. Watanuki**

Group of Medicine, Group of Chemistry*, Group of Physics**, Tohoku University
Sendai, 980 Japan

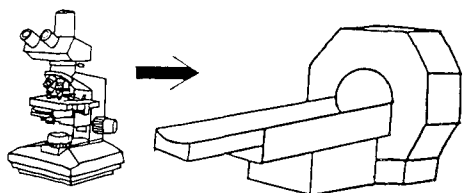
Why PET Now for Cancer Diagnosis?

Schematic representation of the reason why PET now for cancer diagnosis is illustrated in Fig. 1.

At present, final cancer diagnosis is carried out morphologically under the microscope. Since this method is based on the examiner's subjectivity, mistakes are not avoidable. In addition, information on the spreading of cancer cannot be obtained at all. The development of an objective method for cancer diagnosis that provides information on its spreading is eagerly expected.

Using PET, we can obtain quantitative images of the metabolism of viable cells. What is better, the spreading of cancer can be detected easily with PET, because cancer cells can be labelled with positron emitters which irradiate two γ -rays in opposite directions following the extinction of the positron. In addition, if we can distinguish metabolic and histological differences with PET, PET is to be the best method for cancer diagnosis.

Why PET now for cancer diagnosis ?



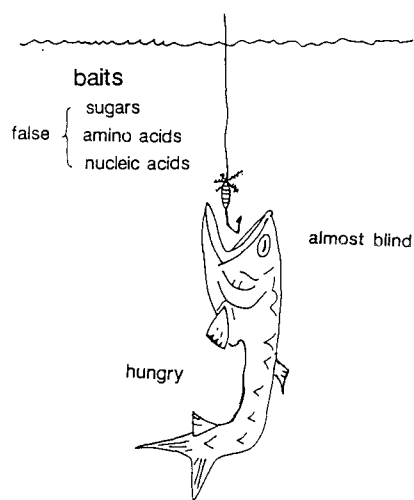
- | | | |
|----------------------------|---|---------------------|
| 1. subjective | → | objective |
| <hr/> | | |
| 2. image | | |
| qualitative | → | quantitative |
| <hr/> | | |
| 3. spreading | | |
| no information | → | information |
| <hr/> | | |
| 4. histological difference | | |
| can be distinguished | → | to be distinguished |
| <hr/> | | |

Fig. 1.

The Direction to Develop Cancer Diagnostic Positron Pharmaceuticals

Schematic representation is illustrated in Fig. 2.

The Direction to Develop Cancer Diagnostic Positron Emitters



T.Matsuzawa

Fig. 2.

In general, cancer cells have two characteristic natures. One is intensive proliferating capacity and the other is undifferentiated character. In other words, cancer cells are hungry for metabolic substrates such as sugars, amino acids, and nucleic acids, because of their intensive proliferating capacity. It is also considered that cancer cells are blind toward metabolic substrates because they lose their selective capacity for these substrates, due to their undifferentiated character.

We can catch starved and blind fish easily with baits! Fishing cancer with baits, such as false sugars, false amino acids and false nucleic acids labelled with positron emitters is our basic idea in developing cancer diagnostic positron pharmaceuticals.

Biological and Clinical Studies of Positron Labelled False Sugars

Pharmaceuticals

As mentioned above, positron labelled false sugars are thought to be good tracers for cancer detection.

The chemical structures of the eight 2-deoxy-2-fluoro-hexopyranoses that belong to the D-series are shown in Fig. 3. The structure of L-glucose derivative is also shown in this figure.

Biological and Clinical Studies of False Sugars

[¹⁸F]-2-DEOXY-2-FLUOROHXOPYRANOSSES

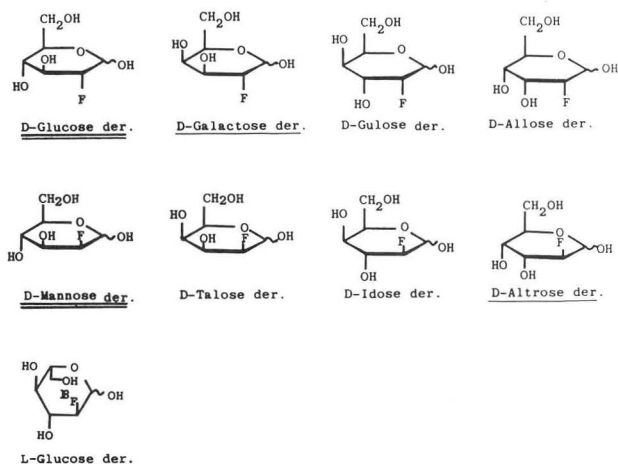


Fig. 3.

Tissue distribution of F-18-deoxyhexopyranoses

Figure 4 (A) and (B) show tissue distribution curves of F-18-deoxyglucose (FDG) and F-18-deoxymannose (FDM) in tumor bearing rats respectively. The tumor uptakes of both agents are very high, they nearly

Tissue distribution of F-18 deoxyhexopyranoses

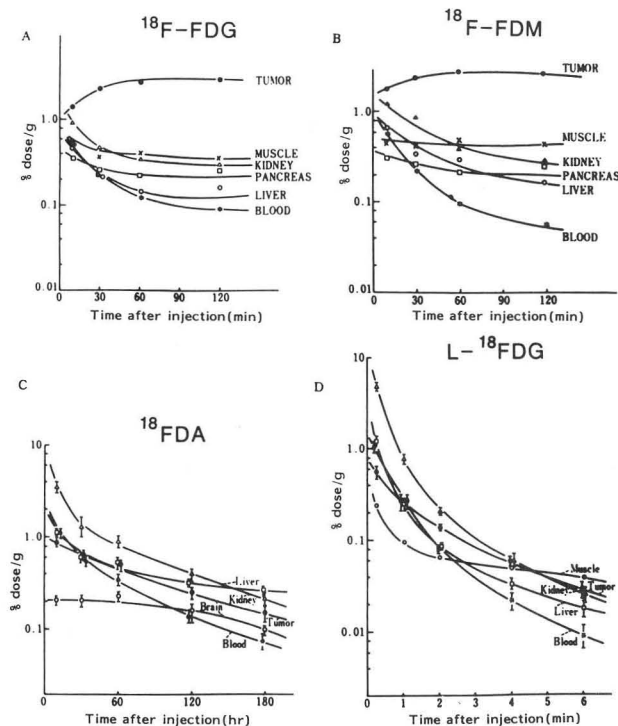


Fig. 4.

reach a plateau 40 min after administration. On the other hand, uptakes of normal liver, kidney, and pancreas are extremely lower than those of the tumors and are followed by rapid washout of radioactivity in spite of high glucose metabolism in these normal organs.

Figure 4 (C) and (D) show the tissue distribution curves of F-18-Altrose (FDA) and L-type-F-18-deoxyglucose (FDG) respectively. The agents are rapidly cleared away from all organs containing tumor tissues.

Both F-18-FDG and FDM, which are physiologically very similar to glucose, they are the most useful agents for cancer detection among the F-18-deoxy-hexopyranoses which we tested. These findings are supporting our basic idea of fishing cancer with baits or with false sugars.

Clinical Study

Figure 5 shows X-CT image of human liver cirrhosis with hepatoma cases. Large low density area was seen in the right lobe. We are not able to distinguish hepatoma in this picture at all.

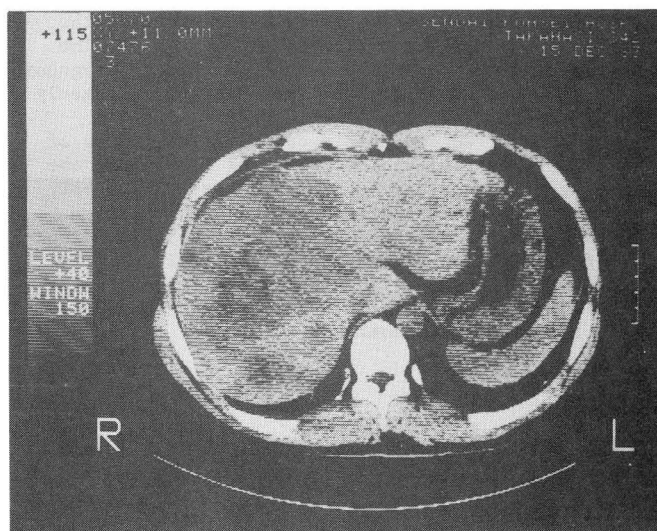


Fig. 5.

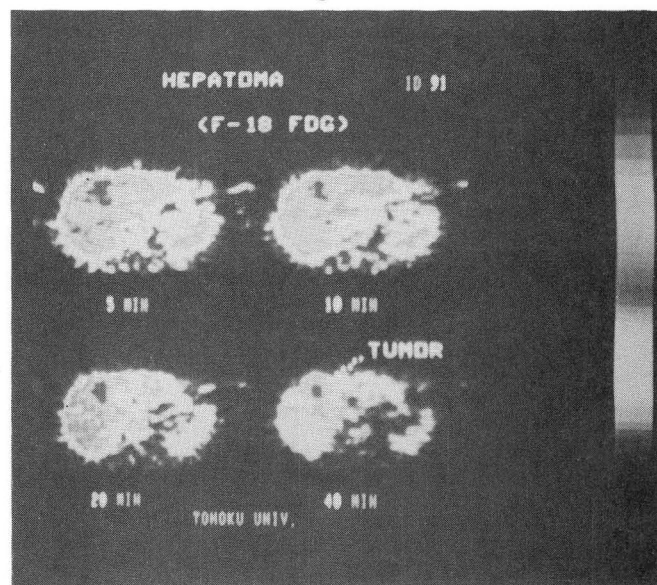


Fig. 6.

Figure 6 shows a sequential tomographic images of F-18-FDG in the same case.

The uptake of normal and cirrhotic liver was initially high, but decreased with time. On the other hand, there was evident increasing of radioactivity in the hepatoma with passing time.

Consequently, we could obtain a clear image of hepatoma 40 min after injection of F-18-FDG.

Time Activity Curves of the Hepatoma and Pancreas Carcinoma with F-18-FDG

3 cases of hepatoma and 2 cases of pancreatic cancer with or without liver metastasis were examined with F-18-FDG by PET. After F-18-FDG injection, sequential scan was performed by PET. Radioactivity in the tissue and tumor was expressed by differential absorption ratio (DAR).

The uptake of normal liver was initially high, but decreased with time. On the other hand, there were increasing of radioactivity in the most tumor cases. The uptake of liver metastasis of the pancreatic cancer is the highest.

However, activity of one of the hepatoma cases was nearly as low as that of normal liver. One of the possible explanation of this low uptake is that the hepatoma might be well differentiated and has less hexokinase activity as that of normal liver.

Therefore, it is considered that degree of the uptake of F-18-FDG is roughly reflecting the malignancy of the tumor.

Time activity curves of ¹⁸F-FDG in hepatoma and pancreas cancers as expressed DAR

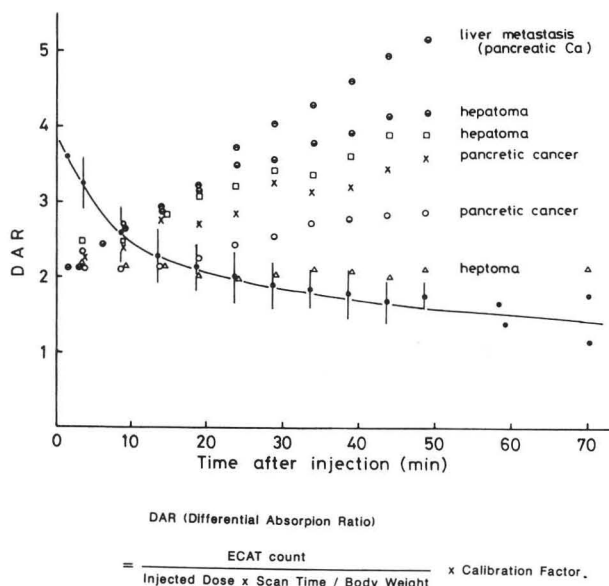


Fig. 7.

Biological and Clinical Studies of Positron-Labelled False and Physiological Amino Acids

For the purpose of finding out the most appropriate amino acid for positron diagnosis of cancer, we compared 11 types of C-11-labelled amino acids and 2 types of N-13-labelled amino acids by examining their uptake into rat tumor in vivo. It was C-11-ACPC, synthesized firstly by Washburn, which showed the highest accumulation in the tumor. The second was C-11-L-Methionine.

Figure 8 shows PET images of human lung cancer with lymph node metastasis after injection of C-11-L-Methionine. We can see many lymph nodes in lung cancer metastasis and its inversion into the thorax. We are able to detect this inversion only with PET.

Figure 9 shows the image of human lung cancer after administration of C-11-Methionine. The tumor is clearly visualized, however, unfortunately normal bone marrow is also visualized, because L-Methionine is a physiological metabolic agent. We are now planning to use the non-physiological amino acid, C-11-ACPC for clinical practice in the very near future.

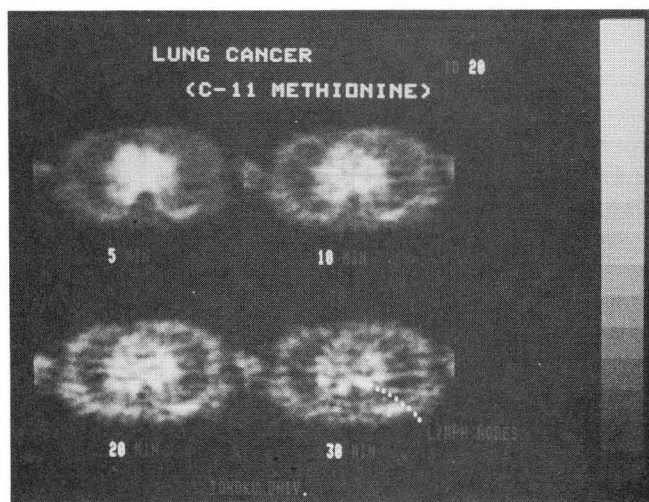


Fig. 8.

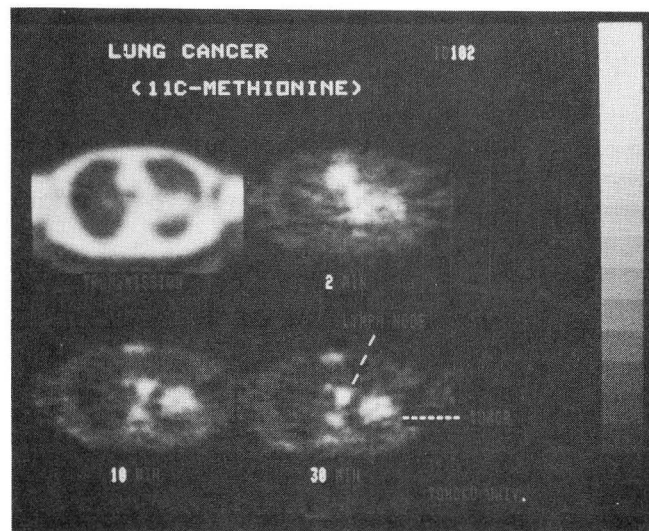


Fig. 9.

Biological and Clinical Studies of Positron Labelled False Nucleic Acids

Tissue distribution and tumor uptake in experimental animal tumors of three F-18-labelled pyrimidines: F-18-FdUR, -5FU, and -FUR, were studied. The tumor-to-organ ratios obtained with F-18-FdUR were always about 3 times higher than those of F-18-5FU and -FUR.

We concluded that F-18-FdUR is a suitable radio-pharmaceutical for tumor imaging among these false nucleic acids.

Figure 10 shows the image of human lung cancer after the administration of F-18-FdUR. The tumor is

Table 1.

Comparative Study of Cancer Diagnosis Using Positron Labelled Amino Acids
Tumor uptake of various radiolabeled amino acids in male
Donryu rats, bearing hepatoma AH 109 A

| Compounds | Rat numbers | Tumor uptake at 20 min. (% Dose/g) | Tumor-to-organ ratio | | | | | |
|---------------------------------------|-------------|------------------------------------|----------------------|-------|-------|-------|-------------|-----------------|
| | | | Blood | Liver | Brain | Lung | Myo-cardium | Skeletal Muscle |
| ¹⁴ N-L-glutamic acid | (5) | 1.34±0.47 | 4.50 | 0.80 | 5.60* | 1.38* | 1.24 | 1.23* |
| ¹⁴ N-L-alanine | (2) | 1.02±0.08 | 2.76 | 0.48 | 3.92 | 0.83 | 0.82 | — |
| → ¹⁴ C-L-methionine | (5) | 2.74±0.36 | 11.40 | 0.60 | 6.33* | 1.93* | 4.70 | 5.38 |
| → ¹⁴ C-D.L-leucine | (5) | 2.20±0.21 | 2.85 | 0.89 | 4.00 | 1.94 | 2.39 | — |
| ¹⁴ C-D.L-valine | (5) | 2.02±0.18 | 1.15 | 0.70 | 2.50 | — | 1.43 | — |
| ¹⁴ C-D.L-phenylalanine | (5) | 1.42±0.25 | 3.32 | 0.77 | 4.43 | 2.03 | 2.67 | — |
| ¹⁴ C-D.L-phenylglycine | (5) | 1.40±0.31 | 2.08 | 1.82 | 5.28 | 1.92 | 2.36 | — |
| ¹⁴ C-D.L-norleucine | (5) | 1.56±0.13 | 2.01 | 1.55 | 3.72 | 1.63 | 1.88 | — |
| ¹⁴ C-D.L-cyclohexylglycine | (5) | 1.24±0.09 | 1.77 | 1.61 | 2.55 | 1.63 | 1.70 | 1.71 |
| → ¹⁴ C-ACPC | (7) | 3.46±0.16 | 4.63 | 2.29 | 4.02* | 3.20 | 3.43 | 3.92 |
| ¹⁴ C-methyl ACPC | (3) | 1.79±0.12 | 2.67 | 2.52 | 3.52 | 2.58 | 2.22 | 2.02 |
| ¹⁴ C-ACHC | (6) | 1.32±0.11 | 1.21 | 1.06 | 3.37 | 1.43 | 1.78 | 2.40 |
| ¹⁴ C-methyl ACHC | (5) | 1.02±0.13 | 1.14 | 1.42 | 3.45 | 1.52 | 1.68 | 1.89 |

*Data from separate experiments.

Table 2.

Biological and Clinical Studies of Positron Labelled False Nucleic Acids

Ratios of Tumor to Normal Tissue in Three ¹⁸F-Pyrimidines

| * | ¹⁸ F-5-FU | | ¹⁸ F-5-FUR | | ¹⁸ F-5-FdUR | |
|--------|----------------------|---------|-----------------------|---------|------------------------|--------------|
| | 30 min | 120 min | 30 min | 120 min | 30 min | 120 min |
| Blood | 1.91 | 5.90 | 2.20 | 6.34 | 2.90 | 18.27 |
| Heart | 1.95 | 4.13 | 2.44 | 5.77 | <u>2.32</u> | <u>11.38</u> |
| Lung | 1.45 | 1.74 | 1.88 | 2.15 | <u>3.20</u> | <u>6.15</u> |
| Brain | 9.22 | 10.63 | 9.73 | 10.85 | <u>19.28</u> | <u>33.50</u> |
| Muscle | 3.36 | 3.61 | 3.57 | 5.16 | 4.59 | 17.13 |
| Spleen | 1.73 | 2.35 | 1.75 | 2.72 | 1.52 | 1.20 |
| Liver | 0.16 | 0.49 | 0.16 | 0.53 | 0.26 | 1.01 |
| Kidney | 0.05 | 0.14 | 0.06 | 0.11 | 0.11 | 0.64 |

clearly visualized 10 minutes after the administration.

It is thought that the uptake of F-18-FdUR is reflecting the degree of cell proliferation.

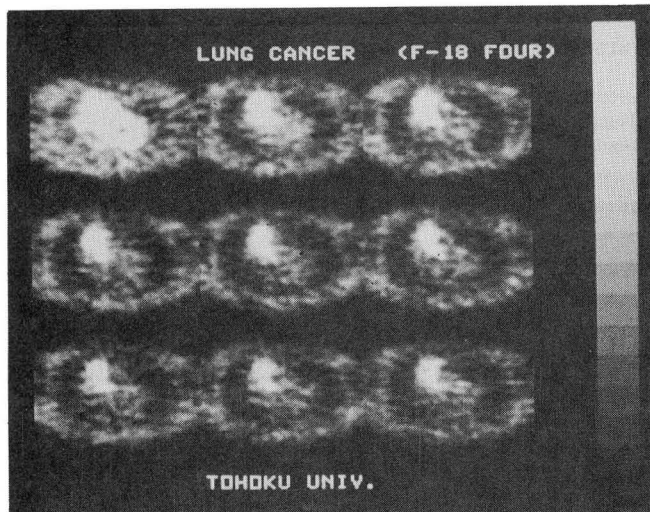
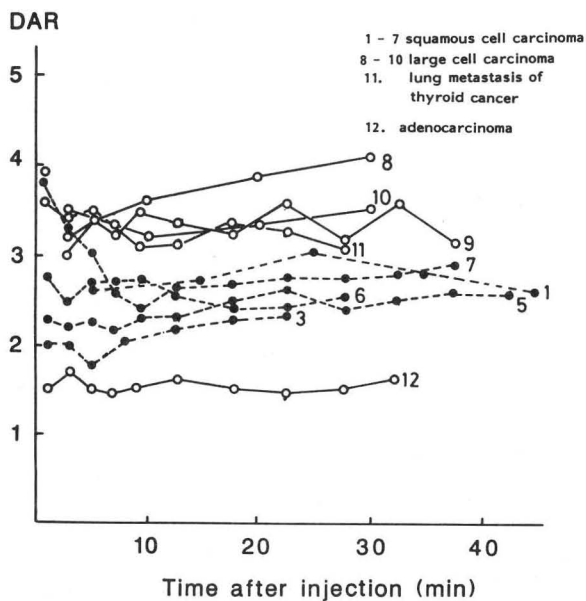


Fig. 10

Relationship between Metabolism and Histology in Lung Cancer

Figure 11 shows the degree of uptake of C-11-methionine into human lung cancer as a function of time.

Uptake of ¹¹C-Methionine in lung cancer



$$\text{DAR (Differential Absorption Ratio)} = \frac{\text{ECAT count}}{\text{Injected Dose} \times \text{Scan Time} / \text{Body Weight}} \times \text{Calibration Factor}$$

Fig. 11

- 1-5 squamous cell carcinoma
- 6-8 large cell carcinoma
- 9 adenocarcinoma

The highest uptake was by large cell carcinoma followed by squamous cell carcinoma and adenocarcinoma had the least uptake. We are able to distinguish histological differences of cancer cells with PET.

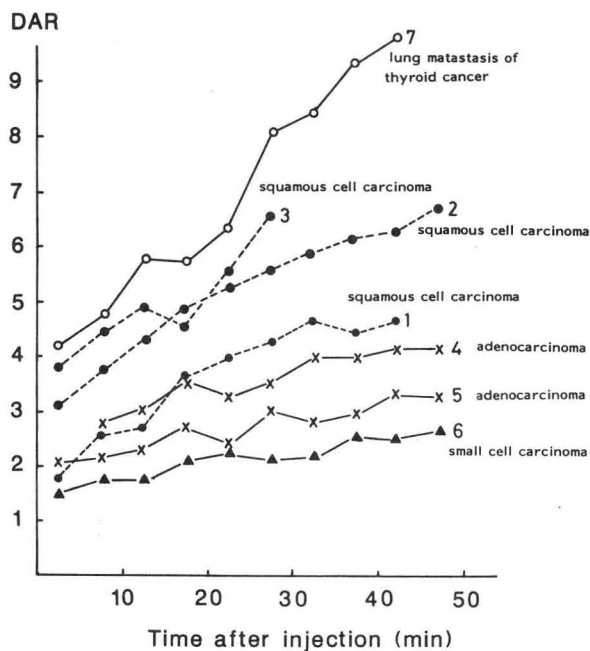
Figure 12 shows the degree of the uptake of F-18-FDG into human lung cancer as a function of time.

- 1-3 squamous cell carcinoma
- 4-5 and 8-9 adenocarcinoma
- 6 small cell carcinoma
- 7 thyroid cancer

The highest uptake was by the thyroid cancer, the next was by squamous cell carcinoma, followed by adenocarcinoma, and the least was by small cell carcinoma.

Using these two positron pharmaceuticals in combination, it is possible to classify various histological types of cancer according to their metabolism. Moreover, if F-18-FdUR is used in addition to these positron-labelled pharmaceuticals, confidence in the diagnosis of histology will become even higher.

Uptake of ¹⁸F-FDG in lung cancer



$$\text{DAR (Differential Absorption Ratio)} = \frac{\text{ECAT count}}{\text{Injected Dose} \times \text{Scan Time} / \text{Body Weight}} \times \text{Calibration Factor}$$

Fig. 12.

Conclusion

Using positron pharmaceuticals in combinations of two or of more, we are able to make clear characteristics of cancer cells by their metabolism and to draw up a protocol for rational treatment.

Our basic idea: "fishing cancer with baits" is very simple, but we believe it is fruitful.